

## COMPARISON BETWEEN MEASURED AND CALCULATED UNDERWATER PRESSURE OF MERCHANT SHIP

JAN BIELAŃSKI<sup>1</sup>, KAROL LISTEWNİK<sup>2</sup>

<sup>1</sup>Gdansk University of Technology  
Narutowicza 11/12, 80-233 Gdansk, Poland  
jbielan@pg.gda.pl

<sup>2</sup>Polish Naval Academy  
Śmidowicza 69,81-103, Gdynia  
k.listewnik@amw.gdynia.pl

*From 2012 The Polish Naval Academy take part in an international research project SIRAMIS, carried out in the framework of the European Defence Agency. The objective of this project is to improve the understanding of ship signature interaction with multi influence sensors in relevant and realistic scenario's. This paper describes selected results of the comparison results of sea trials and model calculations of the hydrodynamic field distribution around a moving ship in selected waters of The Gulf of Gdansk. Despite the good results of the comparison of calculations and measurements of pressure signature for the example of a passenger ship, some measurements deviate significantly from the theoretical results. Due to the lack of reproducibility of these deviations may be due to errors in reading the real positions of underwater measurement modules. This comparison allows for increasing the reliability of theoretical calculations by the results of measurements, and it is expected that the development of this method allows for determining the parameters of the pressure under the hull at any point situated at a distance of not more than 1 meter from the seabed.*

### INTRODUCTION

Hydrodynamic field study design of commercial vessels were carried out under the European Defence Agency SIRAMIS project (investigations were provided in years 2012-2015) in two ways: as an experimental and a theoretical research [1]. Planned and carried out the experiment allows for comparing the results obtained using both methods. Measurements of pressure signatures in marine conditions were provided using made in Polish Naval Academy underwater measuring modules made in Poland called IGLOO and mini-IGLOO [2,

3]. Configuration of measuring equipment during testing is shown in Figure 1. The merchant vessels were using this system.

During the measurement campaign over 60 ships were measured during more than 120 runs over measurement modules. All results presented in this article are based on works which have been carried out under the SIRAMIS project. The partial results were presented previously include a general description of the method of calculation [4] of the pressure signature and examples of comparisons between the results obtained from the measurements and calculations made depending on the type of research ships and tug vessel [5].

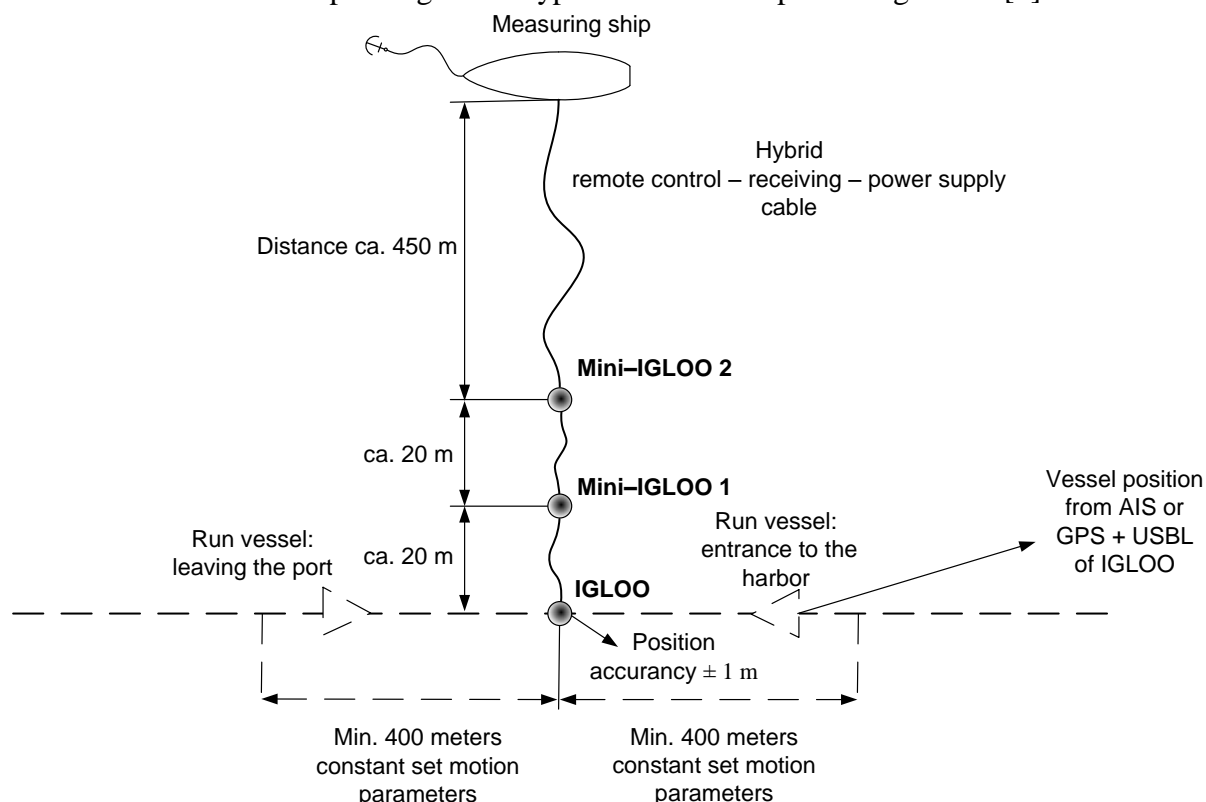


Fig.1. Plan of the signature pressure measurements with a marked the planned deployment of IGLOO's equipment.

### 1. DESCRIPTION OF THE ANALYSIS METHOD AND RESULTS

Previous articles [4, 5] discussed the comparison between theoretical calculations and measurements derived from a single pressure sensor. This paper presents the results obtained from three pressure sensors positioned in three different locations for a type passenger ship hereinafter described as Ship 03.

The depth of the seabed at the place of sensors deployment and their depth are shown in Table 1.

Tab.1. Water depth and dipping sensor during sea trial

Measurement module	Water depth	Dipping sensor
IGLOO	20.85	19.85
mIGLOO2_1	20.50	19.99
mIGLOO2	20.57	20.07

The results of measurements are shown in the set of measurements made for the Ship 03 runs on the Gdynia traffic-lanes to the port. Ship 03 was moving toward the west to the harbor with velocity  $v = 13.5 \text{ kn} = 6.9 \text{ m/s}$ . The main dimensions of ship are: length  $L = 176 \text{ m}$ , maximum width  $B = 30 \text{ m}$  and draft level of ship  $d = T = 6.75 \text{ m}$ . In Table 2 are shown minimum values of HPF as a function of the CPA (Closest Point of Approach). As an example, the record pressure signature measured by the measuring module mini-IGLOO 2 is shown in Figure 2. Fig. 3 shows the pressure signature Ship 03 HPF calculated using BEM the boundary element method in this same CPA (horizontal distance from sensor to the plane of symmetry of the vessel). It can be seen the characteristic shape of the hydrodynamic field passenger vessel equipped with a bulbous bow can be seen to lowers the pressure signature in front of the ship. In previous articles it was presented no analyses of a bulbous bow. The next figure (Fig.4.) represents a cross-section ship hydrodynamic field tested within the CPA = 4.5 m from the plane of symmetry of the ship. The lateral distribution of the pressure field in place of the lowest negative pressure is shows by blue line in Figure 5. The hydrodynamic fields HPF sections of the Ship 03, calculated by BEM, along the plane of symmetry of the ship PS CPA distances equal to AA = 4.5 m, AB = 19.04 m, AC = 21.9 m respectively, and in the plane of symmetry PS of the vessel at the vessel's speed  $v = 6.9 \text{ m/s}$  is presented in figure 6.

Tab.2. Comparison of the results of the measurement and the calculation method of the HPF

Measurement module	CPA [m]	HPFexp_min [daPa]	HPFcalc_min [daPa]	Differences [%]	$Fh = \frac{v}{\sqrt{gH}}$ (H/T)
Calculation	0	-	-485.4	0	0.7 > 0.49 ≈ 0.5 (3.04 < 4)
Mini-IGLOO 2	4.5	-469.4	-463.2	1,32	
Mini-IGLOO 1	19.0	-471.2	-344.2	26,95	
IGLOO	22.0	-318.8	-315.0	1,19	

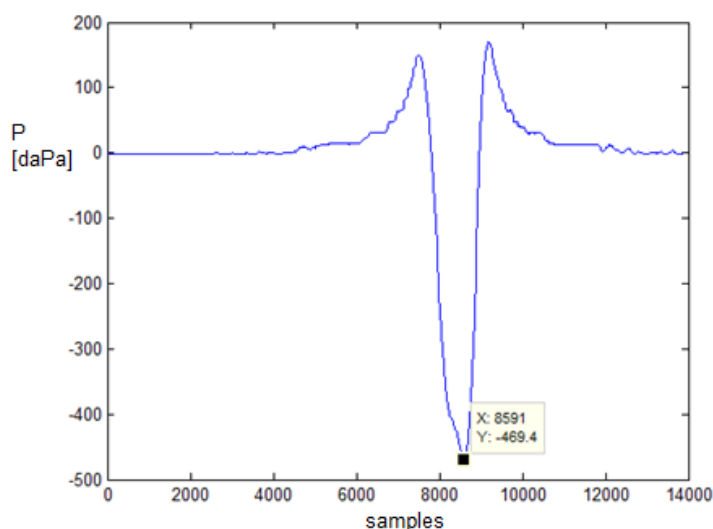


Fig.2. Pressure signature measured by the measuring module mini-IGLOO 2, CPA = 4.5 m.

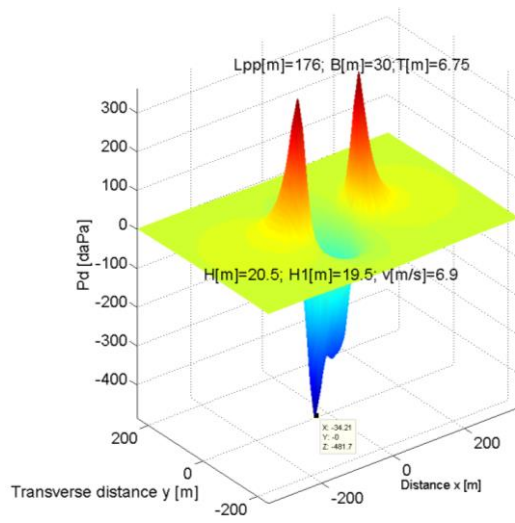


Fig.3. Pressure signature of Ship 03 HPF calculated using BEM the boundary element method, CPA = 4.5 m.

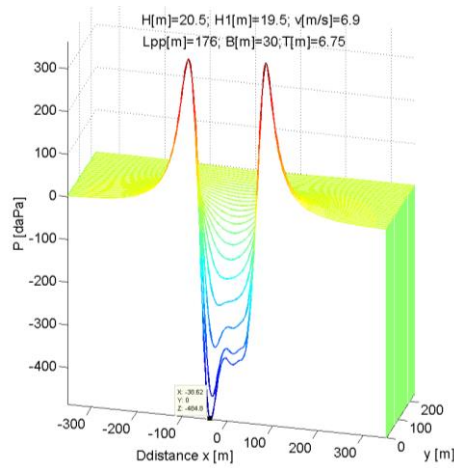


Fig.4. A cross-section hydrodynamic field of ship tested within the CPA = 4.5 m from the plane of symmetry of the ship.

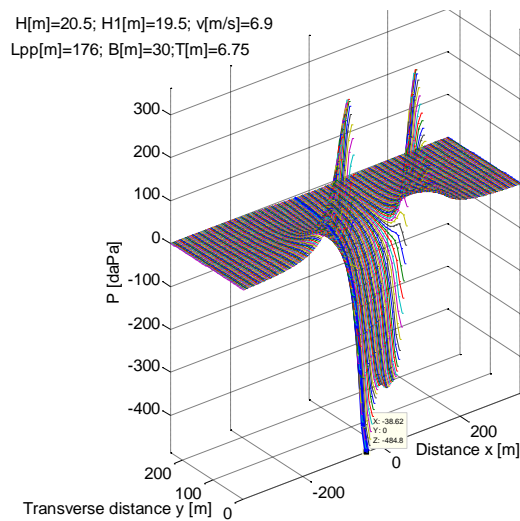


Fig.5. A cross-section hydrodynamic field of ship tested blue line shows the lateral distribution of the pressure field in place of the lowest negative pressure.

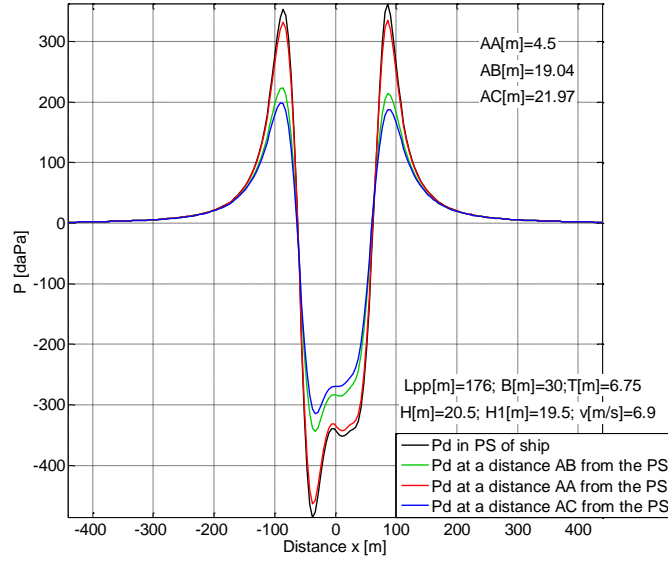


Fig.6. The pressure fields HPF sections of the Ship 03, calculated by BEM, along the plane of symmetry of the ship PS respectively CPA distances.

As it is shown in Figure 7 measurement of the pressure signature is significantly different from the values calculated at point Aexp, located at a distance of CPA = 19.04 m. After recalculating the HPF field to a dimensionless value by dividing the previous value by the dynamic pressure and by dividing the HPF value itself for the point Aexp by  $q_1 = \frac{1}{2} * \rho * (v + 1.18)^2$ , the point Aexp approaches the curve of the calculated values. This may indicate the existence on the edge of the ship's bottom the vortex-generating average speed values of approximately 1.18 m/s in a plane perpendicular to the flow. Estimating the intensity of the  $\Gamma$  (circulation of velocity) by the pressure difference  $\Delta p_d$  measured and calculated by BEM based on the following:

$$\Delta p_d = \frac{1}{2} \rho v^2 = \frac{1}{2} \rho \frac{rot(\vec{v}) \Delta S}{4 \pi} \quad (1)$$

vortex intensity can be estimated using the value:

$$\Gamma = rot(\vec{v}) \Delta S = 4 \pi v^2 \quad (2)$$

such that  $\Gamma = \sim 18.1 \frac{m^2}{s}$  and the resulting average speed of rotation is equal to approx. 1.2 m/s. It is similar to the size of 1.18 m/s of the estimated numerically point shift Aexp in Fig. 7. Based on the above estimation of the intensity of vortex made for the Ship 03 moving at a speed of 6.9 m/s, the resulting estimate of velocity for the ship will be higher, that is,  $v = 7.25$  m/s. The value of the intensity of vortex can reach the value  $\Gamma = \sim 19.74 \frac{m^2}{s}$  and average speed spin 1.25 m/s.

Thus, for all the vessels we have a situation of significant impact on the shallow water flow around the ship, while the impact is greatest for the largest ship. In any case, the value of  $F_h = 0.7$  is for all  $H/T < 4$ . Also a big influence on the flow around the hull of the ship was very uneven seabed.

The calculation was performed by the boundary element method BEM with sources. This model does not generate vortices. It is possible to obtain them with BEM with dipoles or a vortex surface on the surface of the hull, the latter method used for calculation in the case of airfoils. Also, one could check the possibility of calculating using computational fluid dynamics CFD, but in this method there are some problems with the generation of free vortices [6, 7].

It should be emphasized that good compatibility calculations with the measurements provided a slight excess  $F_h = 0.5$  and  $H/T = 4$  the impact of which is moderate in shallow water. Increasing the value of  $F_h$  and decreasing the value of  $H/T$  also gives good compliance calculations with the measurements with other measurements made under the SIRAMIS project, for example, those relating to several general cargo ships on the West part of Baltic Sea or the hydrographic ship in the Gulf of Gdansk. However, in the recent study of the seabed it was relatively smooth. For such seabed in the vicinity of Gdynia despite the known shape of the surface, which is a kind of dump spoil grounds etc, it is it is very difficult to take account of this shape in the calculation HPF regardless of the method to be used.

In conclusion, the results of calculations for ship 03 and results of measurements all runs for ships 03 were collected in Figure 8 and 9 in a dimensionless form. Hydrodynamic pressure is divided by the dynamic pressure  $q = \frac{1}{2} * \rho_0 * v^2$  and the distance the probe from the PS CPA by the length of the ship.

The curves in approximating the results of the experiment and calculated without taking account of the vortex are close to one another while taking into account the effect of the vortex overlap in the range of up to about 50 percent of the width of the ship from the PS.

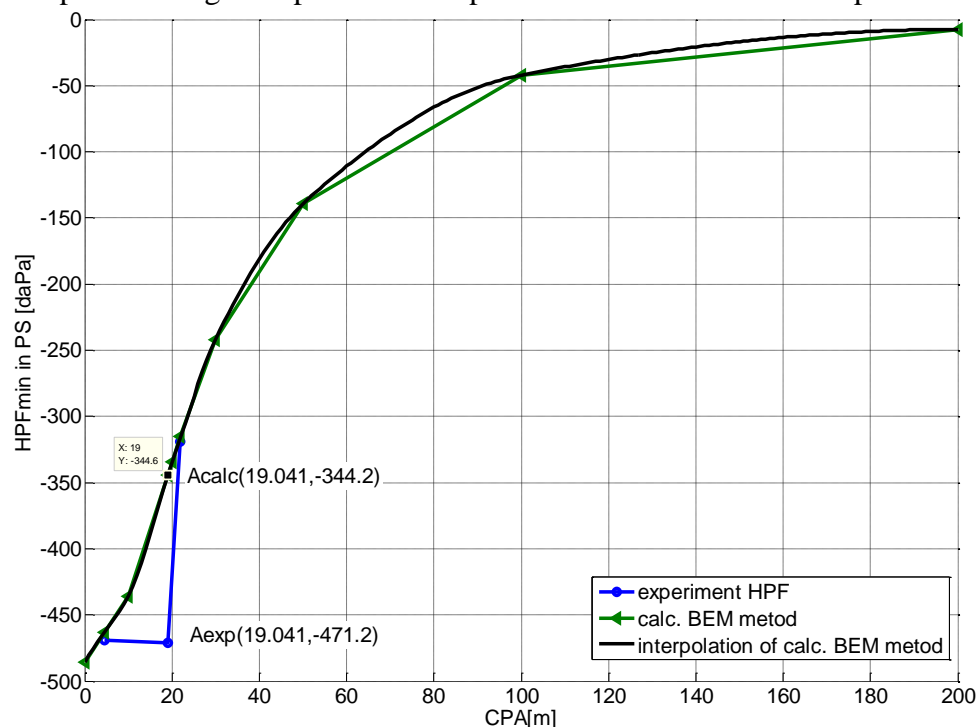


Fig.7. The minimum pressure value of HPF as a function of the CPA for the ship Ship 03, calculated by BEM and measured by IGLOO system.

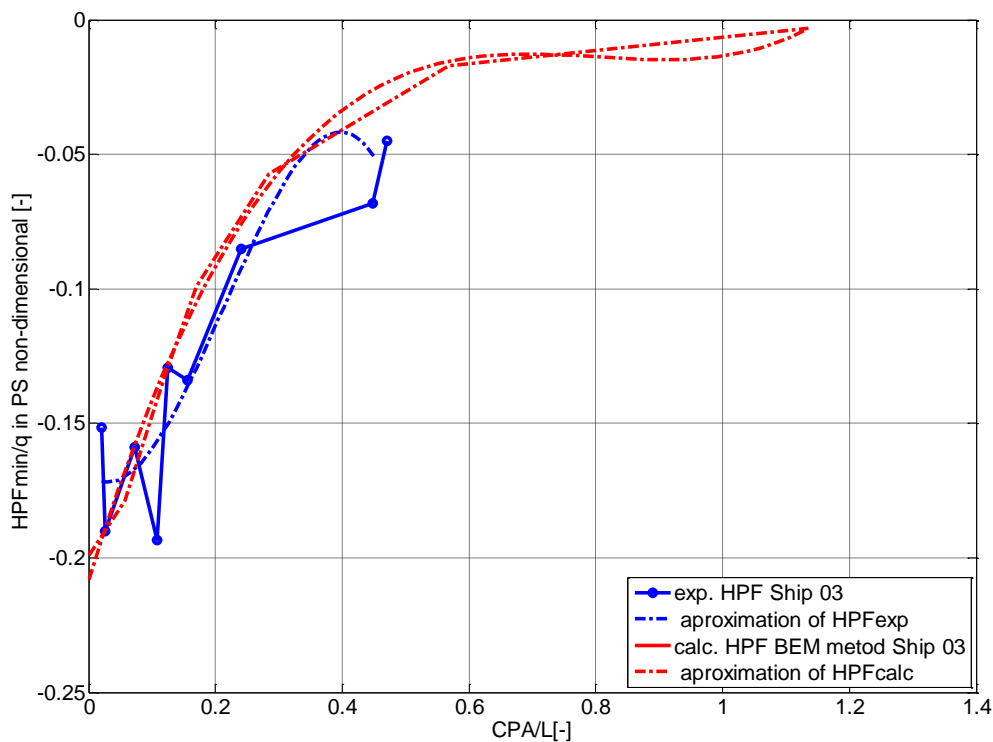


Fig.8. The measured data and calculated pressure fields HPF for Ships 03 in dimensionless form and their third-degree polynomial approximations.

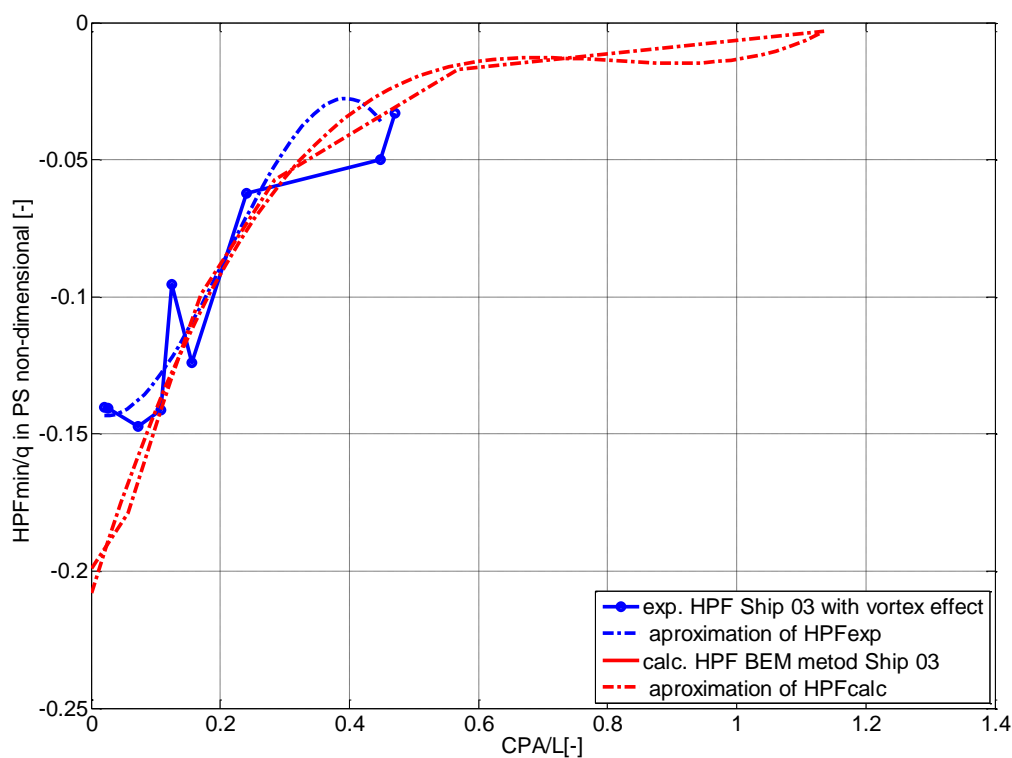


Fig.9. The measured data and calculated pressure fields HPF for Ships 03 in dimensionless form including the impact of vortex on the experimental results and their third-degree polynomial approximations.

## 2. CONCLUSIONS

1. Measurements of the hydrodynamic pressure field (HPF) for large commercial vessels with a length of about 200m made in the shallow sea at a depth of  $H = 20\text{m}$  with a very uneven bottom surface (the area is kind of dump dredging spoils of the port of Gdynia).

2. Calculated and measured distributions of the minimum hydrodynamic pressure (HPF) in a plane perpendicular to the plane of symmetry of the vessel (PS) for larger depths of the sea have the shape of an exponential tending to zero with increasing distance of the CPA which is the distance from the PS.

3. HPF distributions calculated for shallow water (see Figures 3, 4, 5 and 7) also have an exponential shape. In contrast, the measurement results HPF<sub>min</sub> for certain values of the CPA differ from the calculations - are decreasing instead of increasing with increasing distance of the CPA. This is illustrated in Figure 7, with point A<sub>exp</sub> located within the CPA equal to 19m from the PS of ship. The remaining measurement points for other CPA values correspond to the calculations.

4. It should be emphasized that similar results were obtained for several runs of the ship, and that this measurement (point A<sub>exp</sub>) was always performed by the module Mini-IGLOO 1. The above-discussed point was near the area at the side of the ship - half the width of the ship is within the CPA = 15m.

5. These differences between the results of calculations and measurements can have several causes:

A - Can it be the case that a strong vortex is formed by the shallow sea bottom around the bilge part of the ship side, the so-called bilge vortex, generated a large vacuum at the bottom of the ship caused a significant increase in the average flow velocity due to the reduction in flow area by the shallow bottom; the main parameter that describes this phenomenon is the ratio of the depth of the sea to the draft of the vessel  $H/T$ ;

B - A change in the shape of the wave on a free surface around the ship changes the fields HPF in the lower hemisphere around the ship when a vessel's speed ( $v_s$ ) approaches the critical speed of propagation of the wave in shallow water  $v_{\text{crit}} = \sqrt{gH}$  whose ratio determines the so-called depth-related Froude number  $Fh = \frac{v}{\sqrt{gH}}$ , where  $H$  is the depth of the sea; after reaching a value of  $Fh = 1$  bow and stern waves are orthogonal to the PS of the vessel, the second amplitude is lower;

C - The placing of a measuring unit in such a cavity bottom, whereby the pressure wave is reflected from the walls of the cavity increases the HPF<sub>min</sub>;

6. Analysis of the impact on HPF of the bilge vortex (section 5A):

If the average speed on the bottom section A<sub>exp</sub> increased by the value of 1.18m/s, this would indicate the point on the calculated exponential curve;



An attempt estimate the intensity of the vortex by determining the velocity of circulation in the vortex of equations (1.2) gives a value of approximately  $18\text{m}^2/\text{sec}$  allowing the estimate the average speed of rotation to attain the value of  $1.2\text{m}/\text{sec}$ , which is close to the value of  $1.18\text{m}/\text{sec}$  specified above on the basis of the difference between calculated and measured at the point of Aexp;

The value of  $H/T = \sim 3$  for the above measure, which corresponds to medium deep water; the increase in the resistance of the ship for this value is less than equal to 10%;

The results above indicate a high probability that the existence of the bildge vortex significantly increases the vacuum at point Aexp;

7. Analysis of the impact on the HPF of a change in the shape of the surface wave (section 5B):

For Ship 03 the depth Froude number  $F_h = \sim 0.5$ ; if its value belongs to the interval  $[0.4;0.75]$  following: an increase in the angle of propagation of oblique waves; an increase in the amplitude of oblique waves and the waves perpendicular to the direction of ship movement, and an increase in resistance. These phenomena therefore affect the growth of the vacuum hydrodynamic field HPF and result in an increase in the impact area of the field in a direction transverse to the PS. The HPF exponential curve as a function of the CPA becomes flatter at least in close proximity to the vessel.

8. Analysis of the impact on the HPF position measurement module in a cavity of the sea bottom or the existence of another curtain in close proximity to the module (section 5C):

Measurements have not been carried out in close proximity to the bottom of the module Mini-IGLOO-1 and therefore we cannot make any estimation of environmental influence on the measurement module; it is known from observing a diver approaching a sea bottom containing various items such as concrete slabs or barrels, that the probability of environmental influence on the measurements is non-negligible.

9. To summarize, given the impact of various phenomena in the difference measurement and calculation of a HPF at a point at the bottom having CPA value close to half the width of the vessel:

There is a significant probability that the difference resulted in the generation of a bilge vortex with a corresponding impact on the measurement.

Due to relatively high value of the depth Froude number ( $F_h=0.5$ ), it can be determined that there is a significant probability that this difference affected the change in the wave generated by the ship.

The difficulty of taking into account the enviromental impact of the sea bottom on the module increases the probability of error in calibrating the measuring module.

10. The main conclusion in comparing the results of measurements and calculations of hydrodynamic pressure field HPF using the boundary element method is their excellent

compatibility, as shown in Figure 7, with the exception of one measuring point made by the module Mini igloo-1 indicated in Figure 7 as Aexp.

Based on the analysis presented in an article in October this year it was decided to recalibrate the measuring devices of all national teams participating in the second part of the research program of physical fields of ships Siramis II under the auspices of the European Defence Agency - EDA.

This material is based upon work in SIRAMIS Project supported by the European Defence Agency under Contract No A-919-ESM1-GP.07.

## REFERENCES

- [1] K. Listewnik, I. Gloza, J. Bielański, R. Józwiak, Pressure signature analysis - Final report of EDA SIRAMIS Project, Gdynia, 2014.
- [2] I. Gloza, K. Buszman, K. Listewnik, The passive module for underwater environment monitoring, Proceedings of 11<sup>th</sup> European Conference on Underwater Acoustics ECUA 2012, pp. 1787-1793 Edinburgh, UK, 2012.
- [3] K. Listewnik, Underwater noise generated by merchants ships in coastal waters of the Gulf of Gdansk, Proceedings of 43<sup>rd</sup> International Congress on Noise Control Engineering INTER-NOISE 2014, pp. 4184-4190, Melbourne, Australia, 2014.
- [4] J. Bielański, Signature of hydrodynamic pressure field, Hydroacoustics, vol. 15, pp. 13-20, Gdansk, 2012.
- [5] J. Bielański, The hydrodynamic pressure field of the ship Zodiak, measurements and calculations, Hydroacoustics, vol. 17, pp. 17-28, Gdansk, 2014.
- [6] S. S. Rao, The Finite Element Method in Engineering, 3rd ed., Butterworth Heinemann, Boston, 1999.
- [7] O. C. Zienkiewicz, and Taylor, R. L., The Finite Element Method, 4th ed., Vol. 1, McGraw-Hill, London, 1989.